Appendix A

1. Links to the construction summary and LWD data obtained in test pit design

1. Pit 1 Construction and testing timeline and summary:
   https://umd.box.com/s/blgz8pzs80xqs15u2mx38jhvwea5cdix
2. Pit 2 Construction and testing timeline and summary:
   https://umd.box.com/s/sah9335wpegbyzo77abjp8qd9xfd1qni
3. Pit 3 Construction and testing timeline and summary:
   https://umd.box.com/s/mker7qaufdgmpe59g80x7hio4ij7rp1w
4. Dynatest LWD Data_ Pit 1:
   https://umd.box.com/s/qrv939kbdqexg7xwtmj7vl8zrcwrwqso
5. Dynatest LWD data_ Pit 2:
   https://umd.box.com/s/3cm8vpsc4zinvnkp2qchy413l3zyslnn
6. Dynatest LWD data_ Pit 3:
   https://umd.box.com/s/vyzjps3k8r0d6ciirv7urik4vrrr3qq9
7. Olson LWD data_ Pit 1 to 3:
   https://umd.box.com/s/ds8n2zk1arzaqzked3i1or670czyshdw
8. Zorn LWD data_ Pit 1 to 3:
   https://umd.box.com/s/989qpm6u6astu1fvvai09wz9jaho4nq5

2. Pre-construction Laboratory Preparation and Testing

Material characteristics

In this chapter, the properties of the materials used in the test pits are described.

The three materials used in this study included (1) a well graded aggregate base commonly used in state of Virginia designated as VA21a stone (2) a non-cohesive silty sand subgrade soil which was the local subgrade soil used at the TFHRC accelerated loading facility (ALF), referred to in this study as ALF soil; and (3) a cohesive high plasticity clay (HPC) subgrade soil referred to as HPC soil in this study. The ALF soil used in the study was excavated from a hill at TFHRC and the VA21a stone and HPC were donated by Luck Stone Company. The Unified Soil Classification and Atterberg Limits (AASHTO T-89 and T-90) of the studied soils are summarized in Table 0-1.

Table 0-1. Material description

Material	Subgrade/Base	Soil classification	Plasticity Limit	Liquid Limit	Plasticity Index
[-]		[-]	[%]	[%]	[%]
VA21a	Base	GW	-	-	-
ALF	Subgrade	SM	27	31	5
HPC	Subgrade	CH-MH	38	65	27

Figure 0.1 shows the gradation of the materials. The gradations were obtained according to AASHTO T-27 for VA21a and according to AASHTO T-11 and T-27 (wet and dry sieve analysis) for the ALF and HPC soils. The gradations were monitored throughout the phases of the project to ensure uniformity.

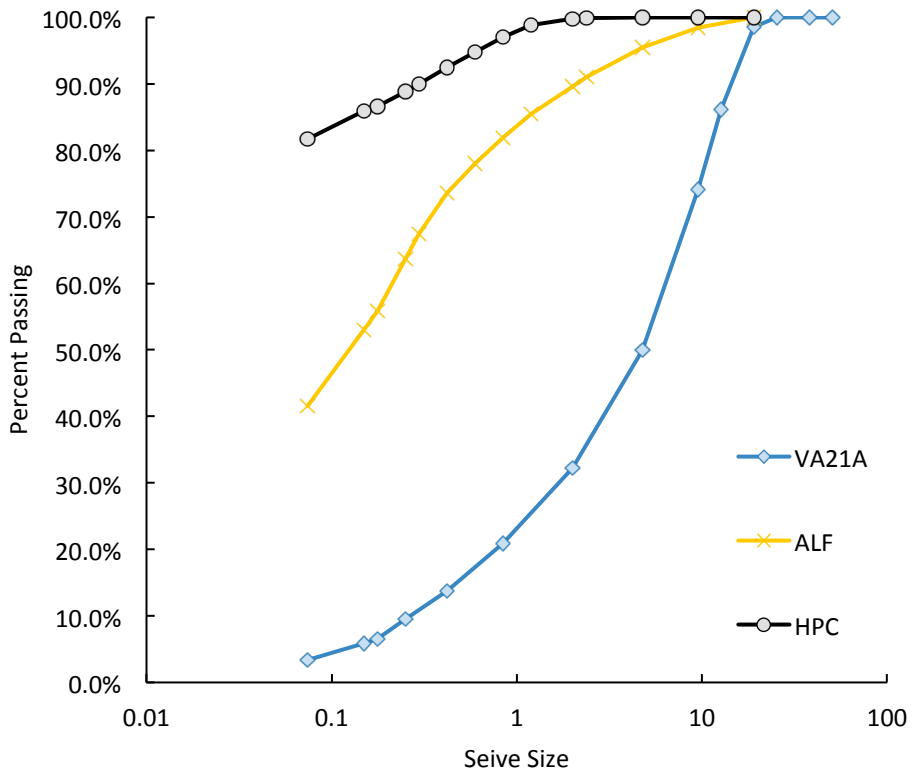

Figure 0.1. Gradation of the materials used in this study

The moisture-density relationships were determined for all three materials. Table 0-2 presents the optimum moisture content (OMC), maximum dry density (MDD) and bulk specific gravity of the test material. Figure 0.2 presents the moisture- density curves for all soils.

Table 0-2. OMC, MDD and Specific gravity of the test material

Soil Type	AASHTO Procedure	Method	Compaction energy	MDD	OMC	Specific Gravity(1)
[-]	[-]	[-]	[-]	kg/m^3 (pcf)	[%]	[-]
VA21a	T-99	D	Standard	2307.7 (144.0)	5.0	2.77
VA21a	T-180	D	Modified	2435.9 (152.0)	4.5	
ALF	T-99	C	Standard	1923.1 (120.0)	11.5	2.71
ALF	-	C	Semi Modified(2)	2003.2 (125.0)	10.5	
ALF	T-180	C	Modified	2083.3 (130.0)	9.5	
HPC	T-99	A	Standard	1522.4 (95.0)	24.0	2.66

(1) Specific gravity test according to AASHTO T-84 and T-85
(2) Customized compaction energy: 3 layers, 25 drops per layer using a 4.54 kg rammer and a 457 mm drop

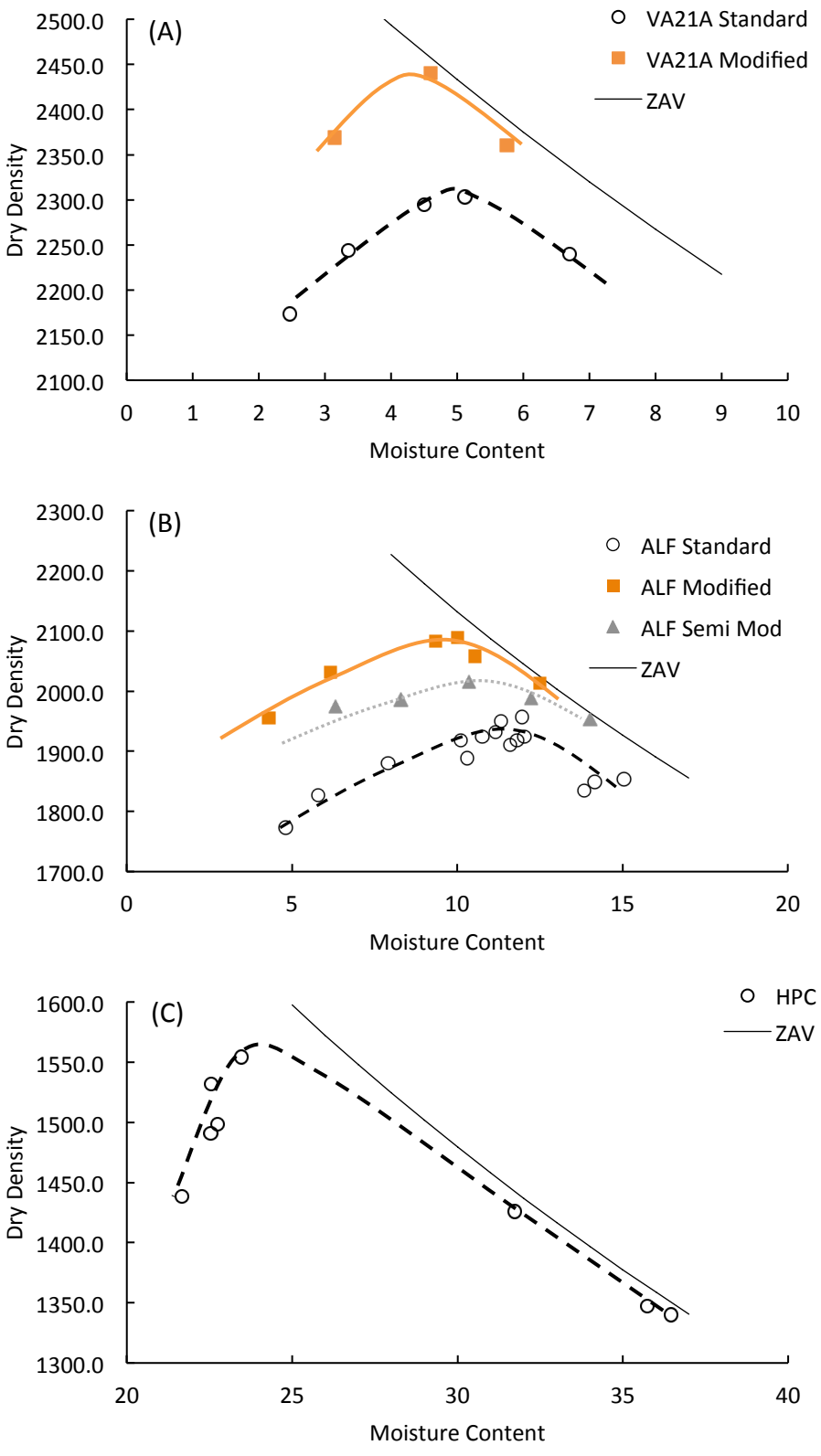

Figure 0.2. Moisture- Density relationships for (A) VA21a, (B) ALF, and (C) HPC.

Ohaus MB45 moisture analyzer

Moisture content is one of the main factors influencing soil modulus. The ability to quickly measure the soil moisture content in field is of particular importance. The Ohaus MB45 moisture analyzer shown in Figure 0.3 was evaluated for the purpose of quick moisture measurements during the pits construction.

The Ohaus MB45 moisture analyzer is basically a scale accompanied by a halogen dryer unit to quickly dry the soil samples.

The Ohaus MB45 moisture analyzer determines the moisture content of practically any substance. The instrument operates on the thermogravimetric principle. First, the moisture analyzer determines the weight of the sample; then the sample is quickly heated by the integral halogen dryer unit and moisture vaporizes. During drying, the instrument continuously determines the weight of the sample and displays the results as % moisture content, % solids, weight or % regain. The MB45 takes about 15 minutes to dry the samples.

Ohaus MB45 Moisture Analyzer was evaluated against oven-drying measurements for four different kinds of soil—gravel, sand, silty sand, and clayey sand. For each soil, 20 to 26 tests at various moisture contents were tested.

The results showed a very high correlation (R = 0.98) between the moisture contents measured using the two techniques for all evaluated soils. The moisture content measured by MB45 was generally slightly lower (by a factor of approximately 0.9) than the moisture measured using the standard oven drying technique.

Results from the evaluation are shown in Figure 0.4. The MB45 was found to be a robust device, especially for fine soils. A few drawbacks of the MB45 are its low capacity (45 gr), which makes it less suitable for larger aggregates, and the need for a generator to power the device in the field.

The correction factor of 1.11 can be applied to correct for the underestimation of MB45. For higher accuracy, a soil-specific calibration can be developed.

Figure 0.3. Ohaus MB45 moisture analyzer

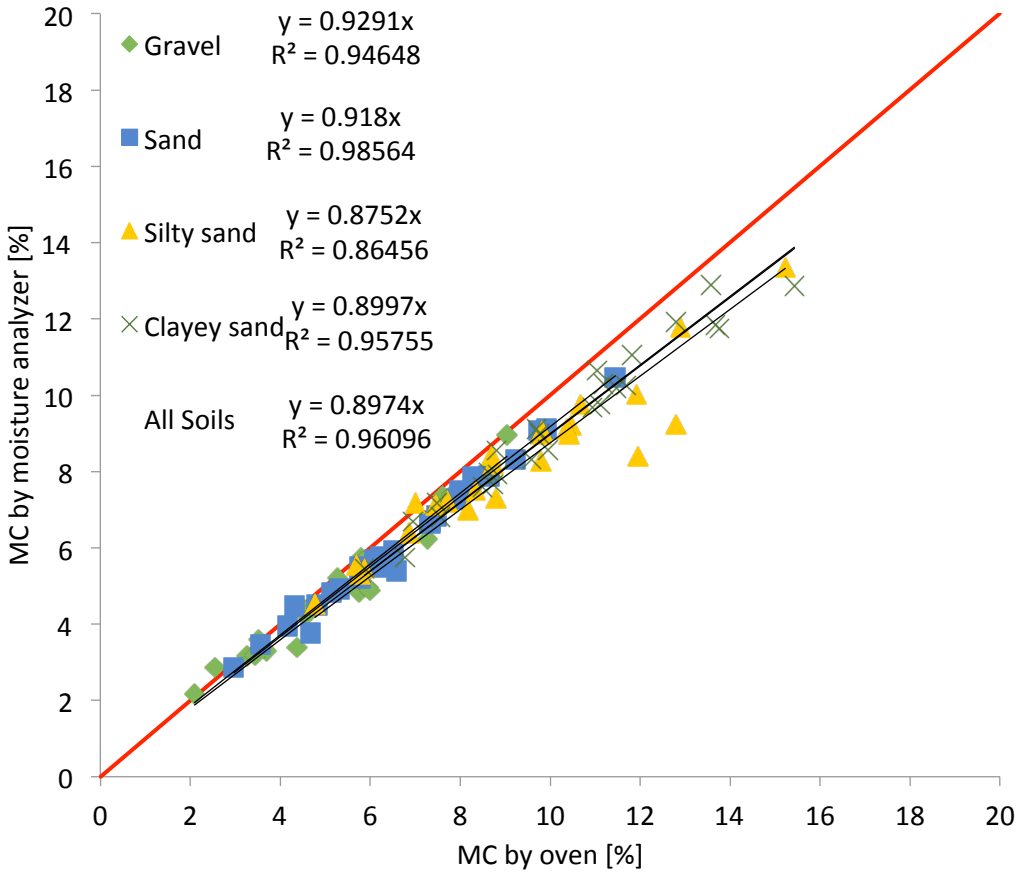

Figure 0.4. Comparison of water content measurement by Ohaus MB45 moisture analyzer and oven drying for gravel, sand, silty sand, and clayey sand soil.

Resilient Modulus Testing

The M_R tests were performed at similar moisture and density conditions as during the test pit construction as well as at optimum conditions.

The number of layers and drops per layer were adjusted for the taller M_R mold, which has a height to diameter ratio of 2, in order to achieve a similar compaction energy similar to that of the Proctor test. Table 0-3 lists the adjusted numbers of layers and drops per layer used in compaction of the M_R samples unless otherwise stated (e.g., case of less than standard or poor compaction for ALF Pit 1).

Table 0-3. The mold dimensions, number of layers and drops per layer for proctor molds and M_R molds for standard and modified compaction energy

Proctor Mold		Standard (T-99)		Modified (T-180)	
		100 mm mold	150 mm mold	100 mm mold	150 mm mold
Weight of the hammer	[kg]	2.495	2.495	4.54	4.54
Height of drop	[mm]	305	305	457	457
Number of drops per layer	[-]	25	56	25	56
Number of layers	[-]	3	3	5	5
Diameter of mold	[mm]	101.6	152.4	101.6	152.4
Height of mold	[mm]	116.3	116.3	116.3	116.3
Volume of mold	[cm^3]	0.94	2.12	0.94	2.12
Compaction energy/volume	[kNm/m^3]	594	591	2698	2686
M_R Mold		**Standard**		**Modified**	
		100 mm mold	150 mm mold	100 mm mold	150 mm mold
Weight of the hammer	[kg]	2.495	2.495	4.54	4.54
Height of drop	[mm]	305	305	457	457
Number of drops per layer	[-]	26	48	31	59
Number of layers	[-]	5	9	7	12
Diameter of mold	[mm]	101.6	152.4	101.6	152.4
Height of mold	[mm]	203.2	295.02	203.2	295.02
Volume of mold	[cm^3]	1.65	5.38	1.65	5.38
Compaction energy/volume	[kNm/m^3]	589	599	2681	2678

Table 0-4 summarizes the testing plan for the M_R testing performed in the lab.

Table 0-4. Testing plan for M_R testing

Soil Type	Target MC	Target DD	Mold diameter	Compaction energy	Condition	# of Replicate
[-]	[%]	[kg/m^3 (pcf)]	[mm]	[-]	[-]	[-]
VA21a	4.5	2435 (152)	150	Modified	Optimum- Pit 2, Pit 3	2
ALF	11.5	1922.2 (120.0)	100	Standard	Optimum	3
ALF	11.5	1922.2 (120.0)	100	Standard	Optimum- After 4 hrs drying	2
ALF	15.3	1837.3 (114.7)	100	Standard	Pit 2	2
ALF	10.0	1771.2 (110.6)	100	<standard	~Pit 1	2
ALF	7.3	1670.7 (104.3)	100	<standard*	~Dry	1
HPC	24.0	1521.8 (95.0)	100	Standard	Optimum	2
HPC	29.0	1457.7 (91.0)	100	Standard	Pit 3	2

* 3 layers- 15 drops per layer

Table 0-5, Table 0-6, and Table 0-7 summarize the average test results for the HPC, VA21a and ALF soils respectively. The individual results for each test sample are provided in Appendix 9.

Table 0-5. HPC M_R test results

Test Condition/ Material	[-]	OPT	Pit 3
Achieved MC	[%]	24.5	30.8
Achieved DD	[pcf]	93.6	89.4
	[kg/m3]	1499.2	1432.1
Pa	[kPa]	101.3	101.3
k1	[-]	888.8	583.4
k2	[-]	0.378	0.095
k3	[-]	-0.843	-1.789
SSE	[MPa^2]	2261.6	259.0
Sqr(SSE)	[MPa]	47.56	16.09
R^2	[MPa^2]	26.8	81.0
R^2_adj	[MPa^2]	16.4	78.3
Max Sample-to-Sample CV of M_R at a given stress state	[%]	6.4	18.7
Average Sample-to-Sample CV of M_R at a given stress state	[%]	2.4	5.3

Table 0-6. VA21a M_R test results

Sample ID	[-]	VA21a__Ave OMC
Achieved MC	[%]	3.7
Achieved DD	[pcf]	153.4
	[kg/m3]	2458.0
Pa	[kPa]	101.3
k1	[-]	590.6
k2	[-]	0.824
k3	[-]	0.000
SSE	[MPa^2]	2765.0
Sqr(SSE)	[MPa]	52.58
R^2	[MPa^2]	96.6
R^2_adj	[MPa^2]	95.7
Max Sample-to-Sample CV of M_R at a given stress state	[%]	47.9
Average Sample-to-Sample CV of M_R at a given stress state	[%]	17.6

Table 0-7. ALF M_R test results

Sample ID	[-]	OPT	OPT_4 hr	Pit 2	~Pit 1	~ Dry
Achieved MC	[%]	11.9%	11.3%	14.6%	9.4%	7.3%
Achieved DD	[pcf]	118.9	119.0	116.5	110.6	104.3
	[kg/m3]	1904.3	1906.0	1867.0	1771.2	1670.6
Pa	[kPa]	101.3	101.3	101.3	101.3	101.3
k1	[-]	1437.4	927.1	177.6	793.9	1233.4
k2	[-]	0.429	0.232	0.485	0.601	0.313
k3	[-]	-3.717	-2.257	0.000	-2.023	-3.212
SSE	[MPa^2]	131.6	209.2	384.1	1635.8	818.1
Sqr(SSE)	[MPa]	11.5	14.46	19.60	40.44	28.6
R^2	[MPa^2]	98.1%	89.2%	58.7%	66.2%	83.5%
R^2_adj	[MPa^2]	97.6%	86.5%	52.8%	61.4%	79.1%
Max Sample-to-Sample CV of M_R at a given stress state	[%]	32.5%	52.8%	27.9%	5.0%	-
Average Sample-to-Sample CV of M_R at a given stress state	[%]	16.2%	29.6%	13.2%	1.8%	-

Instrumentation and Calibration

The test pits were instrumented with 6 thermocouples, 6 volumetric water content (VWC) sensors, and 2 earth pressure cells to record the environmental and load-related responses during the time of construction and testing.

Data acquisition system and software

The data acquisition system shown in Figure 0.5 included an NI SCXI-1001 (Signal Conditioning eXtensions for Instrumentation) compact 12-slot chassis housing NI SCXI- 1600 USB Data Acquisition and Control Module, SCXI- 1102 (32-channel thermocouple amplifier) module and several SCXI-1520 (8-channel universal strain/bridge) modules.

The sensors were connected to terminal blocks which mounted on the corresponding modules on the chassis. Table 0-8 lists all the modules that the chassis housed with their associated terminal block and sensors connected to.

LabVIEW SignalExpress, an interactive data-logging software was used for quickly acquiring, analyzing, and presenting data from the instruments.

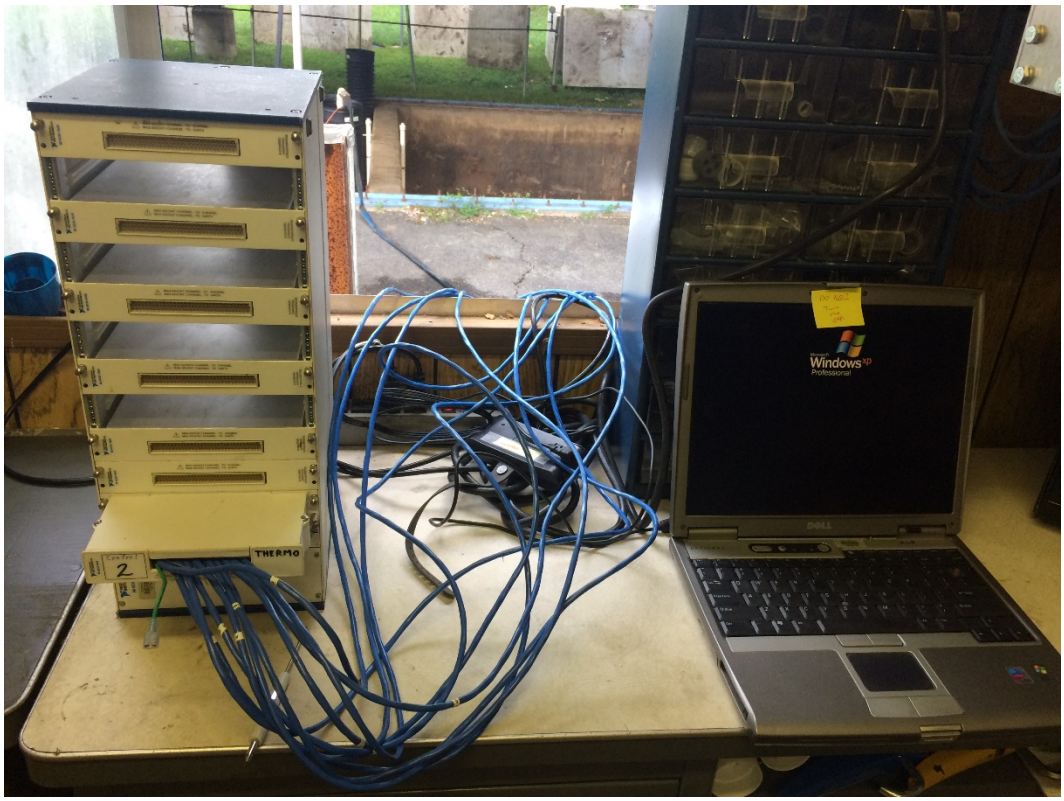

Figure 0.5. NI SCXI- 1001 Rugged, compact 12-slot chassis

Table 0-8. Summary of the modules and terminal blocks used for sensors in the chassis

Module	Terminal block	Sensor
SCXI -1520 (8-Channel Universal Strain/ Bridge)	SCXI -1314	VWC, earth pressure cell
SCXI-1102 (32-Channel Thermocouple Amplifier)	SCXI-1303	Thermocouple

Thermocouple sensors

The Omega EXPP-T-20-TWSH-SLE wire thermocouples consisted of a pair of solid shielded wire (constantan and copper) twisted and soldered (Figure 0.6). The ground wire was folded back as can be seen in Figure 0.6. No lead wire splicing was performed on the thermocouples as they were cut to full required length (15 m each) as shown in Figure 0.7.

Thermocouples were connected to the NI SCXI-1303 terminal block mounted to front of SCXI-1102 module as shown in Figure 0.8.

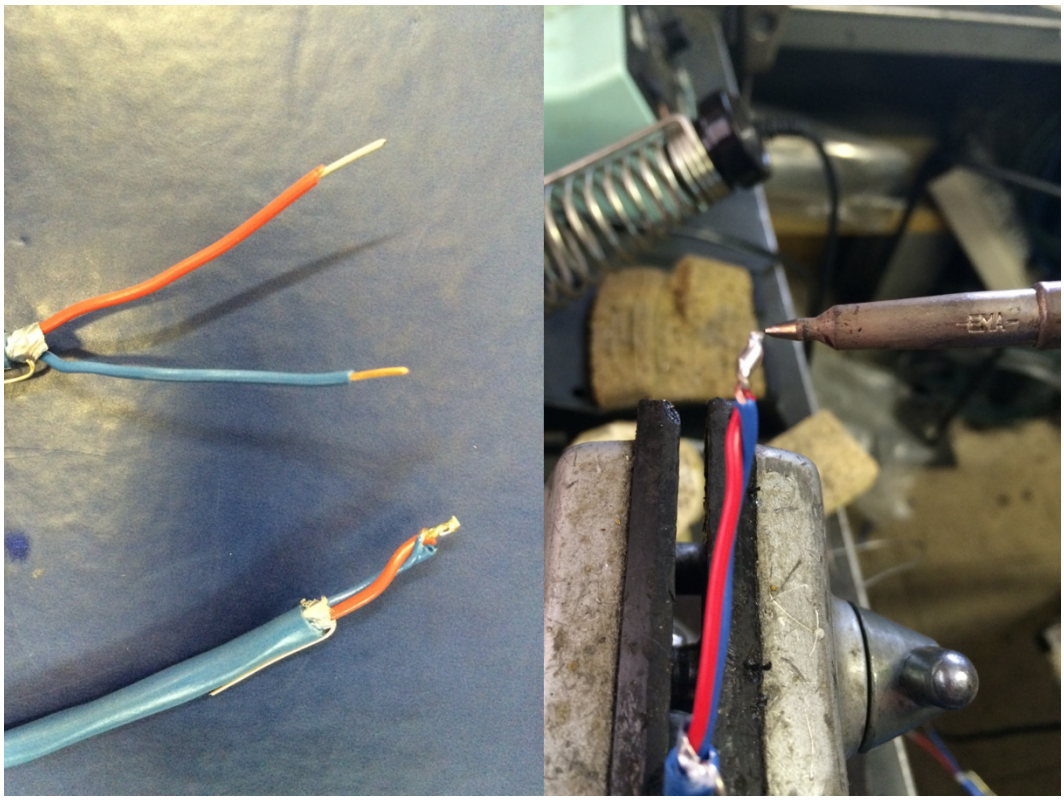

Figure 0.6. Theromcouple fabrication

Figure 0.7. Thermocouple wires cut to length

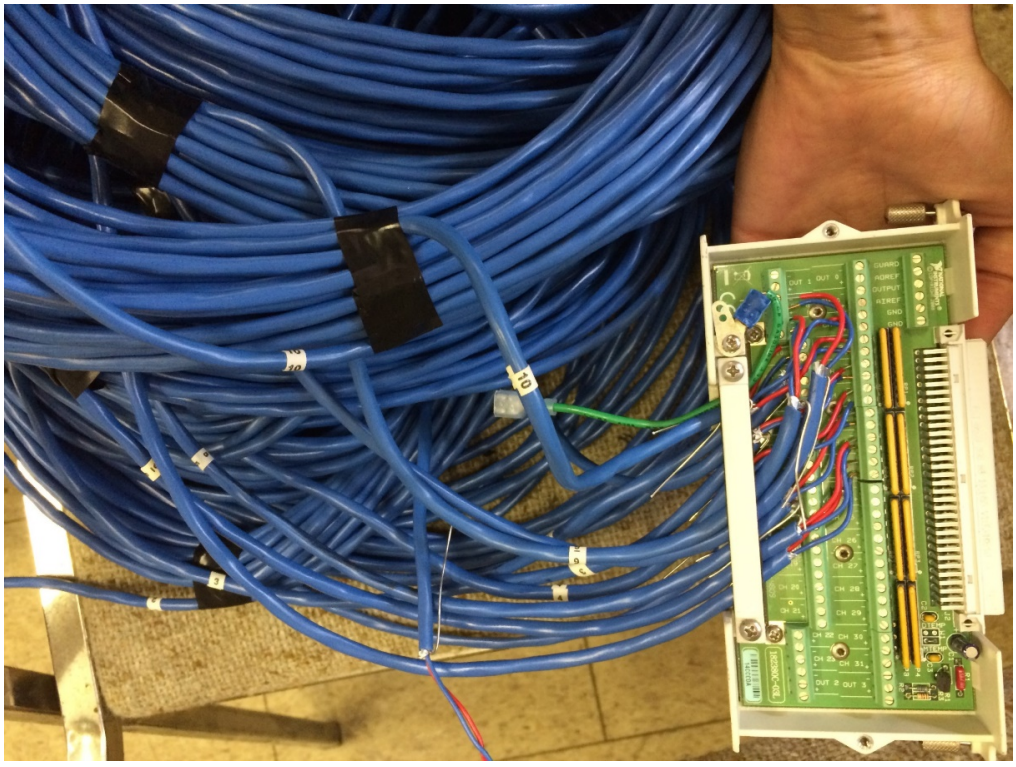

Figure 0.8. Connecting the thermocouples to the NI SCXI 1303 terminal block.

Volumetric water content (VWC) Sensor

VWC in the test pits was measured by Decagon ruggedized GS-1 sensors (Figure 0.9). GS-1 measures the dielectric constant of the soils using capacitance and frequency domain technology.

The dimensions of GS-1 sensor is 8.9 cm x 1.8 cm x 0.7 cm. Its maximum volume of influence is 1430 mL and its zone of influence is shown in Figure 0.10. The default length of the sensors was 5 m and therefore splicing of the wires was performed to accommodate the required length for the test pits.

The GS-1 sensor requires 3 to 15 VDC excitation power. The sensor supplies a 70 MHz oscillating wave to the sensor prongs that changes according to the dielectric constant of the material. The GS-1 measures the charge and outputs a voltage between 1000 mV to 2500 mV (or RAW value) that strongly correlates to the VWC. The output setting being mV or RAW value depends on the data logger. With a non-Decagon data logger such as the NI data acquisition system used for the embedded sensors in the test pits, the output is mV while with ProCheck, the handheld sensor read-out and storage system by Decagon, the RAW value is displayed instead. Therefore two different sets of calibration equations should be used as appropriate. The difference between the two is the slope constant (RAW=1.365*mV).

Laboratory Calibration of GS-1: The factory default calibration of the GS-1 sensor is not relevant to the levels of compaction that is achieved in pavements. Therefore, a soil-specific calibration was performed in laboratory. Samples were compacted at OMC and MDD and ±2% of OMC according to AASHTO T-99—Method C for HPC and ALF soil and according to AASHTO T-180—Method D in case of VA21a aggregate.

The sensor prongs were inserted into top of the soil while still being inside the solid-wall metal Proctor mold. Since the zone of influence of the GS-1 sensor is non-symmetric along its prongs, the sensor was inserted at 7.5 cm radial distance from the center of the mold to maximize the extent of the influence of the sensor inside the soil. ProCheck was used to read the output RAW value. The RAW data was correlated with measured VWC of the soil samples. The constructed linear calibration equations are presented in Table 2-8 for each soil as a function of RAW and mV.

Figure 0.9. Decagon GS-1 ruggedized volumetric water content (VWC) sensor—www.Decagon.com

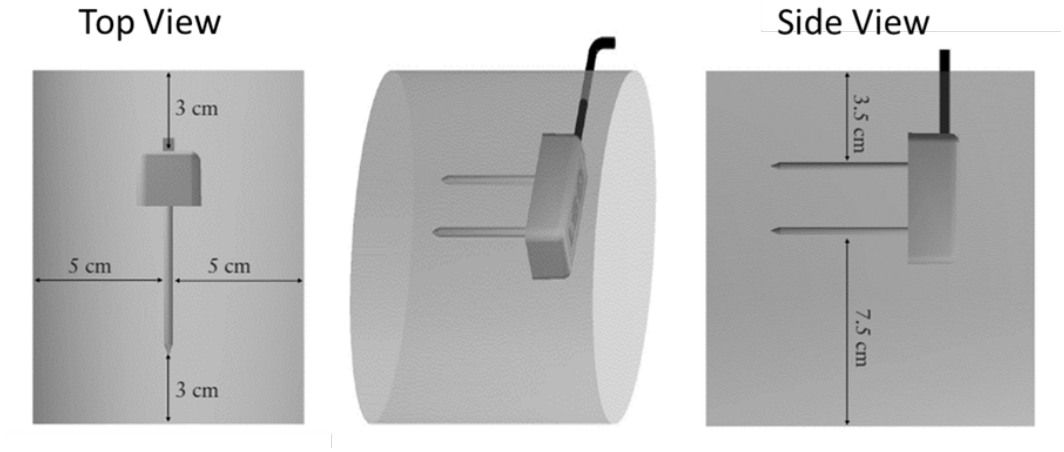

Figure 0.10. The influence zone of GS-1 sensor—GS-1 sensor manual

Figure 0.11. Placement of GS-1 VWC sensor in VA21a aggregate

Table 0-9. Calibration equations for the implemented instrumentations

Device	Calibration equation
Decagon GS-1 Volumetric Moisture Content VMC sensor ($\boldsymbol{\theta}$)	$\boldsymbol{\theta\ VA21a = 1.92E-04 \times mVol - 0.1348}$ $\theta\ VA21a = 1.40E-04 \times RAW - 0.1348$
	$\theta\ ALF = 4.53E-04 \times mVol - 0.539$ $\theta\ ALF = 3.32E-04 \times RAW - 0.539$
	$\theta\ HPC = 3.34E-04 \times mVol - 0.3357$ $\theta\ HPC = 2.44E-04 \times RAW - 0.3357$
Earth Pressure Cell	$\sigma\ (kPa) = 120.0 \times Vol$ $\sigma\ (psi) = 17.4 \times Vol$

Earth pressure cell

Pressure was measured by GEOKON granular materials pressure cell Model 3515 in test pits #1 and 2. The earth pressure consisted of two stainless steel plates welded together around their edges so as to leave a narrow gap in between. The gap is filled with de-aired hydraulic oil. As the two plates get squeezed, pressure builds up in the hydraulic oil. The pressure cell is connected to a transducer that converts the mechanical input, pressure, into an electrical output, voltage, ranging from 0-5 volts. An excitation voltage of 10 VDC was used to power the sensor. Figure 0.12 presents a schematic of earth pressure cell. The calibration equation is provided in Table 2-8.

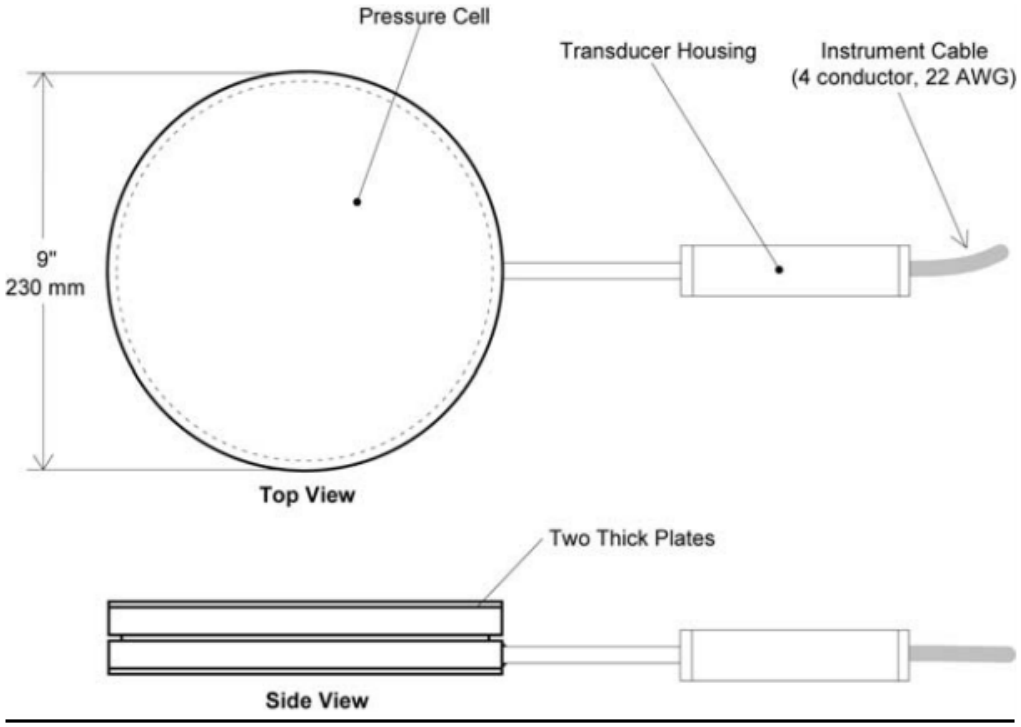

Figure 0.12. Schematic of model 3515 Granular materials pressure cell, Geokon Instruction manual

Figure 0.13. Earth pressure cell

3. Test pit construction

This chapter summarizes the steps that were taken for the construction of the test pits including subgrade, and base layers.

Test pit properties

The test pits at TFHRC were approximately 4.6× 4.6× 2.4 m^3 (15×15×8 ft^3). Half of the depth of the pits (~1.2 m) was already filled with a uniform crushed stone (Figure 0.1). The elevation of each pit was measured at multiple locations inside and across the walls before placing the test material (Table 0-1). The low coefficient of variation (CV) of less than 1.3% indicates the uniformity of the test pits.

Table 0-1. Elevation of pits before material placement

Pit #	Depth of Pit	
	Average	CV
[-]	[cm (in)]	[%]
1	120.5 (47.5)	0.9
2	123.0 (48.4)	1.3
3	120.2 (47.3)	1.1

The test pits were equipped with reaction frame with a pneumatic pulsed loading capability, which was used for static plate load testing. The pits also included infrastructure to control and change the water table. Prior to the construction, water was pumped out of the pits and a geotextile was placed to preserve the existing crushed stones from potential contamination (Figure 0.2).

Figure 0.1. Crushed stone

Figure 0.2. Placement of geotextile on top of the 1.2 m crushed stone.

Design of the test pits

To achieve the objectives of the study, the subgrade and base layers in each test pit were designed to a target moisture, density, and layer thickness. The material used in each pit and the design values for each layer are listed in

Table 0-2.

The ALF subgrade of Pit 1 was designed to be placed at slightly dry of OMC at a target MC of $(-10\% \times OMC)$, which is within the current Moisture-Density based specification limits, but to a lower density of below 90% of the MDD from standard compaction energy.

The ALF subgrade of Pit 2 was designed to be placed at wet of OMC and to the minimum density of 95% of the MDD from standard compaction energy.

Similar to Pit 2, The HPC subgrade of Pit 3 was designed to be placed at wet of OMC and to the minimum density of 95% MDD from standard compaction energy.

The VA21a base of Pit 2 and 3 were designed to be placed at OMC and to achieve 95% MDD from modified compaction energy.

Table 0-2. Target MC, Density, and layer thickness

Pit #	Layer	Material	Moisture condition	Target MC		Target PC*	Target Layer thickness	Sub layers
[-]		[-]	[-]	[%]		[%]	[cm (in)]	[-]
1	Subgrade	ALF	Dry of OMC	10	$-10\%\times OMC$	≤ 90	508.0 (20.0)	3
	Base	-	-	-	-	-	-	-
2	Subgrade	ALF	Wet of OMC	15	$+30\%\times OMC$	≥ 95	609.6 (24.0)	6
	Base	VA21a	At OMC	4.5	OMC	≥ 95	203.2 (8.0)	2
3	Subgrade	HPC	Wet of OMC	29	$+20\%\times OMC$	≥ 95	508.0 (20.0)	5
	Base	VA21a	At OMC	4.5	OMC	≥ 95	101.6 (4.0)	1

*PC= Percentage compaction

Tent setup

A tent was setup on top of the test pits to preserve them from the frequent summer rains during the time of construction and testing and to reduce the potential environmental effects for this large scale controlled-condition testing (Figure 0.3).

Figure 0.3. Tent setup on top of the test pits.

Soil preparations for compaction

The soils were transported and stockpiled in an open area close to the test pits. Figure 0.4 to Figure 0.10 show the soil stockpiles for ALF, HPC and VA21a soils.

Considerations made prior to compaction included regular moisture content checking and consequential wetting or drying of the soils to reach the target moisture condition; removing the organic and and other deleterious materials from the soil—especially in case of the locally obtained ALF soil as shown in Figure 0.4; breaking the very large chunks of the soil—especially in case of the HPC soil as Figure 0.7 and Figure 0.8—using a skid-steer loader and hammer jack; and covering the stockpiles with tarps in case of an anticipated rain (Figure 0.10).

To efficiently dry the soils, skid-steer and backhoe loader were used to spread the soils. In case of the ALF soil used in Pit 1, which was intended to be compacted dry of optimum, the soil for each sublayer was transferred and spread inside the pit and was dried prior to compaction using a portable oscillating fan.

The material for each sublayer—around 7-10 half-full buckets of skid-steer loader with 0.73 m^3 capacity—was transferred to the pits. To expedite the transfer and distribution of the soils in pits, a ramp was made as shown in Figure 0.11. To assure a uniform compaction, extra care was taken to evenly spread and distribute each load of soil poured in the pits using shovels and rakes for ALF and VA21a soil and by hand for chunks of HPC soil prior to compaction. The nominal thickness of the loose layer was 5 cm above the target thickness for ALF and HPC sublayers placed in Pit 2 and Pit 3, and 2.5 cm above the target thickness in case of the VA21a sublayers placed in Pit 2 and 3 and ALF soil sublayers in Pit 1.

Figure 0.4. ALF Stockpile- Removing the organinc soil from ALF soil.

Figure 0.5. Spreading ALF stockpile for drying prior to compaction.

Figure 0.6. Stockpile of HPC soil.

Figure 0.7. Use of hammer jack in breaking the large chunks of HPC soil.

Figure 0.8. Use of skid-steer loader in breaking and spreading HPC for further drying.

Figure 0.9. Stockpile of VA21a stone.

Figure 0.10. Covering the stockpiles.

Figure 0.11. Use of ramp for transferring the material into the pits.

Compaction

The two following compactors were used in the project:

(1) Sheep foot trench roller with remote control (Figure 0.12)

(2) Vibratory plate compactor (Figure 0.13).

The sheep foot trench roller had a drum width of 81.3 cm and weighed 1370 kg. It induced an impact force of up to 62.3 kN.

The plate compactor had a plate size of 50 x 56 cm^2 and weighed 88 kg. It induced an impact force of up to 15 kN.

The sheep foot trench roller was mainly used for compaction of the ALF soil in Pit 2 and the HPC soil in Pit 3. The plate compactor was mainly used for compaction of ALF soil in Pit 1 and the VA21a stone in Pit 2 and 3. The compaction method for each sublayer is listed in Table 0-3, Table 0-4, and Table 0-5 for Pits 1, 2, and 3, respectively. As can be seen, the compaction method and numbers of passes were adjusted to some extent throughout the construction process

to achieve the desired levels of compaction. The construction of each sublayer took around 3 hours to complete.

Figure 0.12. Sheep foot trench roller with remote control.

Figure 0.13. Vibratory plate compactor.

Table 0-3. Construction timeline and compaction procedure for Pit 1.

Lift	Date	time	Compaction method
1	22-Jul	13:30	3 passes of sheep foot compactor with high vibration
2	24-Jul	8:00	2 passes of plate compactor with medium vibration
3	24-Jul	13:00	2 passes of plate compactor with medium vibration

Table 0-4. Construction timeline and compaction procedure for Pit 2.

Lift	Date	time	Compaction method
1	9-Jul	13:00	2 coverages of sheep foot compactor with high vibration
2	9-Jul	16:00	2 coverages of sheep foot compactor with high vibration
	10-Jul	9:00	Additional 2 coverages of sheep foot compactor with high vibration and 1 pass of plate compactor with high vibration
3	10-Jul	13:00	2x2 coverages of sheep foot compactor with high vibration and 1 pass of plate compactor with high vibration
4	10-Jul	16:00	2x2 coverages of sheep foot compactor with high vibration
5	13-Jul	10:00	2x2 coverages of sheep foot compactor with high vibration
6	13-Jul	15:00	2x2 coverages of sheep foot compactor with high vibration
7	14-Jul	13:00	2x2 coverages of sheep foot compactor with high vibration
	14-Jul	14:00	additional 2x2 passes of plate compactor with high vibration
	14-Jul	15:00	Water spray and 6 extra passes of plate compactor with high vibration
8	15-Jul	11:00	2x2 coverages of sheep foot compactor with high vibration and 3 passes of plate compactor with high vibration

Table 0-5. Construction timeline and compaction procedure for Pit 3.

Lift	Date	time	Compaction method
1	17-Jul	11:00	2x2 coverages of sheep foot compactor with high vibration
2	17-Jul	16:00	2x2 coverages of sheep foot compactor with high vibration
3	20-Jul	11:00	3x3 coverages of sheep foot compactor with high vibration
4	20-Jul	15:00	3x3 coverages of sheep foot compactor with high vibration
5	21-Jul	11:00	3x3 coverages of sheep foot compactor with high vibration
6	22-Jul	10:00	2x2 coverages of sheep foot compactor with high vibration and 3 passes of plate compactor with high vibration
	22-Jul	11:00	Water spray and 2 extra passes of plate compactor with high vibration

Nuclear moisture and density measurements

The compaction effort was monitored with a Troxler 3440 nuclear moisture-density gauge (Figure 0.14). The measurements were performed in direct transmission mode (Figure 0.15). In

direct transmission mode, the rod containing the Cesium-137 source is lowered to the desired depth. The detectors in the gauge base measure the radiation emitted by the source rod. This gives an estimate of the average density of the material from the source to the surface.

Table 0-6, Table 0-7, and Table 0-8 summarize the dry density (DD), gravimetric water content (w), percent compaction (PC), and VWC (θ) on each sublayer for Pit 1, Pit 2, and Pit 3, respectively. Nuclear gauge measurements were taken at a minimum of 3 random spots on each sublayer. The measurements on the final sublayer of each layer were taken at the same locations as where the LWD tests were performed, e.g. Figure 0.14 shows the testing performed on the final sublayer of base in Pit 3.

A uniform compaction with very low spatial variability was achieved throughout the construction, as can be inferred from the low CV reported in

Table 0-6, Table 0-7, and Table 0-8.

Figure 0.14. Troxler 3440 Nuclear moisture-density gauge.

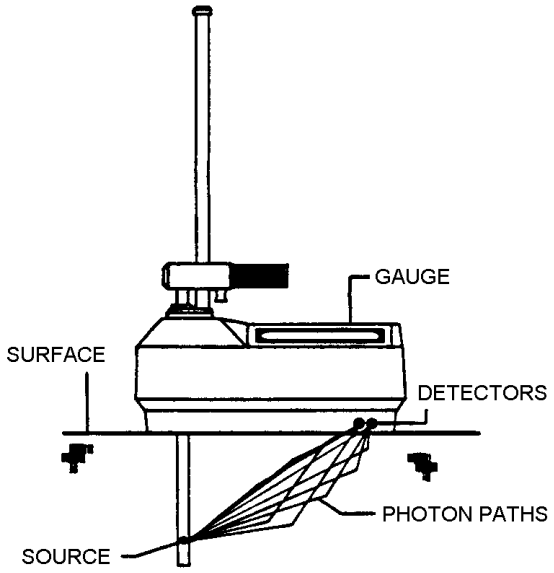

Figure 0.15. Nuclear gauge in direct transmission geometry.

Table 0-6. Nuclear moisture-density test results for Pit 1.

Lift #	Soil type	Penetration depth	Dry density		w		PC	θ	
			Average	CV	Average	Sd	Average	Average	Sd
[-]	[-]	[cm]	[kg/m^3 (pcf)]	[%]	[%]	[%]	[%]	[%]	[%]
1	ALF	10.2	1904.6 (118.9)	-	11.9	-	99.1	22.7	-
2	ALF	15.2	1648.0 (102.9)	3.8	9.7	1.1	85.7	16.0	1.4
3	ALF	20.3	1593.3 (99.5)	1.3	10.2	0.6	82.9	16.2	1.0

Table 0-7. Nuclear moisture-density test results for Pit 2.

Lift #	Soil type	Penetration depth	Dry density		w		PC	θ	
			Average	CV	Average	Sd	Average	Average	Sd
[-]	[-]	[cm]	[kg/m3 (pcf)]	[%]	[%]	[%]	[%]	[%]	[%]
1	ALF	5.1	1800.9 (112.4)	4.3	14.4	1.3	93.7	26.0	2.4
2	ALF	7.6	1809.6 (113.0)	1.8	16.5	0.7	94.1	29.8	0.8
3	ALF	10.2	1836.0 (114.6)	1.8	16.1	0.4	95.5	29.6	0.3
4	ALF	10.2	1874.6 (117.0)	1.4	14.9	0.5	97.5	27.8	0.9
5	ALF	10.2	1879.8 (117.4)	1.8	13.7	0.3	97.8	25.8	0.7
6	ALF	10.2	1834.8 (114.5)	4.2	15.4	0.7	95.5	28.2	1.1
7	VA21a	10.2	2306.3 (144.0)	1.5	5.9	1.6	94.7	13.6	2.9
8	VA21a	10.2	2388.8 (149.1)	4.3	4.7	0.2	98.1	11.2	0.6

Table 0-8. Nuclear moisture-density test results for Pit 3.

Lift #	Soil type	Penetration depth	Dry density		w		PC	θ	
			Average	CV	Average	Sd	Average	Average	Sd
[-]	[-]	[cm]	[kg/m3 (pcf)]	[%]	[%]	[%]	[%]	[%]	[%]
1	HPC	10.2	1408.7 (87.9)	3.3	30.6	2.7	92.6	43.0	2.8
2	HPC	10.2	1485.4 (92.7)	5.3	29.3	3.6	97.6	43.4	2.9
4	HPC	10.2	1450.7 (90.6)	4.4	29.0	3.8	95.3	41.9	3.9
4	HPC	20.3	1497.2 (93.5)	2.1	27.3	2.0	98.4	40.9	3.0
5	HPC	10.2	1419.2 (88.6)	4.0	29.9	1.6	93.3	42.3	2.0
6	VA21a	10.2	2364.6 (147.6)	1.2	3.6	0.4	97.1	8.5	0.9

Layer thicknesses

The final thicknesses of the subgrade and base layer on each pit was measured at multiple points inside and across the walls of the pits as shown in Table 0-9. The thickness of the layers were fairly even throughout the pit area with CV of less than 4%. The highest CV was for HPC soil which was the hardest soil to handle.

Table 0-9. Final Layer thicknesses

Pit	Subgrade		Base	
	Average	CV	Average	CV
[-]	[cm (in)]	[%]	[cm (in)]	[%]
1	50.8 (20.0)	1.1	-	-
2	59.9 (23.6)	2.6	19.3 (7.6)	2.4
3	50.5 (19.9)	4.0	10.7 (4.2)	2.5

Decagon Volumetric Water Content (VWC) measurements

VWC was measured at various locations and sublayers on the ALF, HPC and VA21a soils with GS1 and nuclear density gauges. For the GS1 sensor, the calibration equations listed in Table 0-9 were used. The VWC for nuclear gauge was calculated using the following formula from the measured data:

$$\theta = \frac{w * \gamma_d}{\gamma_w}$$

where $\theta = VWC, \gamma_d = dry\ density, and\ \gamma_w = density\ of\ water.$

Table 0-10 shows the average VWC measured with the two methods. The spatial relationship was poor for a given type of soil as can be seen in Figure 0.16.

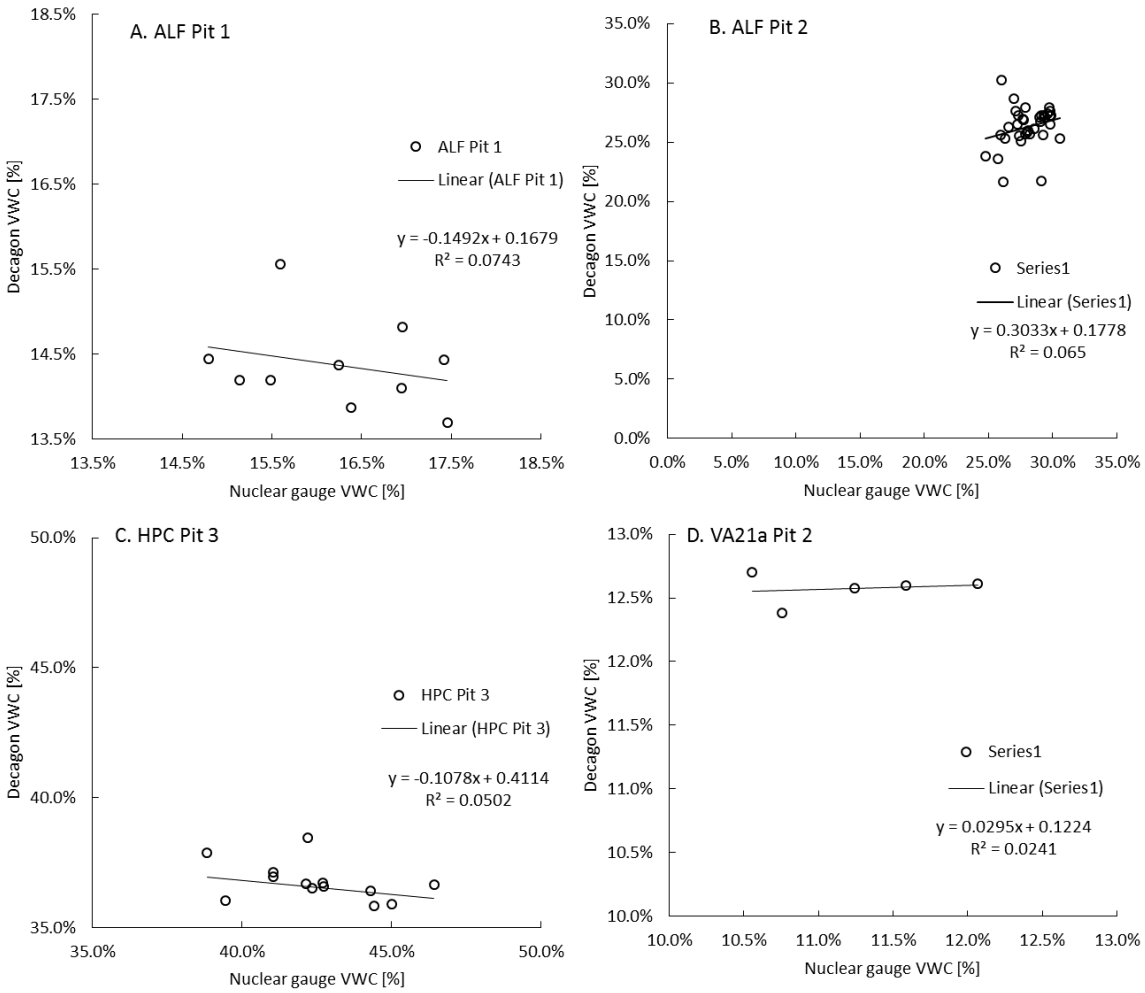

Figure 0.16. Decagon VWC vs. Nuclear gauge VWC for A. ALF Pit 1, B. ALF Pit 2, C. HPC Pit 3, and D. VA21a Pit 2.

However, The VWC of the different soils at different pits were aggregated and distinguishable with the sensor. A strong correlation was found between the two methods shown in Figure 0.17. Decagon sensor slightly underestimated the VWC by the factor of 0.9 on average.

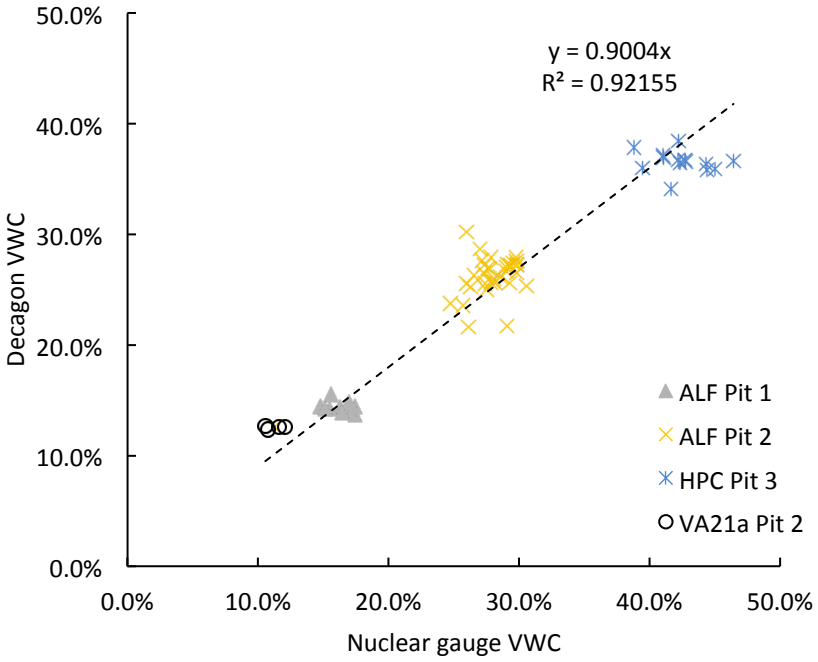

Figure 0.17. VWC measurements: Decagon versus Nuclear gauge.

Table 0-10. VWC as measured by Nuclear gauge and Decagon GS1 sensor.

Pit number	Lift number	Material type	Nuclear gauge VWC		Decagon GS1 VWC	
			Average	Sd	Average	Sd
[-]	[-]	[-]	[%]	[%]	[%]	[%]
Pit 1	Lift 3	ALF	16.2%	1.0%	14.4%	0.6%
Pit 2	Lift 2	ALF	27.1%	0.6%	27.6%	1.2%
Pit 2	Lift 2	ALF	29.8%	0.8%	26.5%	1.1%
Pit 2	Lift 3	ALF	29.6%	0.3%	27.4%	0.3%
Pit 2	Lift 4	ALF	27.8%	0.9%	25.7%	0.6%
Pit 2	Lift 5	ALF	25.7%	0.8%	23.6%	1.8%
Pit 2	Lift 6	ALF	28.1%	1.0%	26.0%	1.6%
Pit 2	Lift 8	VA21a	11.2%	0.7%	12.6%	0.1%
Pit 3	Lift 1	HPC	42.7%	3.4%	36.7%	1.0%
Pit 3	Lift 5	HPC	42.3%	2.0%	36.5%	1.2%

Gravimetric water content (GWC) measurements

Ohaus MB45 MA, and oven drying were used to monitor the GWC of stockpiles, and to control construction quality in conjunction with nuclear moisture-density gauge during material spread and after compaction.

Ohaus MB45 in particular was being evaluated for its feasibility as a tool for rapid moisture measurements. The switch-off criterion which the instrument considers drying as complete and automatically discontinues the measurement process was specified as “less than 5 mg weight loss in 60 ms”.

It took about 10-13 minutes to completely dry the VA21a aggregate. The drying time was about 20-23 minutes for the ALF and 60-70 minutes for the HPC soil.

There was a good correlation between the GWC measured by the Ohaus MB45 and the nuclear moisture-density gauge after applying the 1.11 correction factor to MB45 as previously obtained in laboratory. Figure 0.18 presents the comparison.

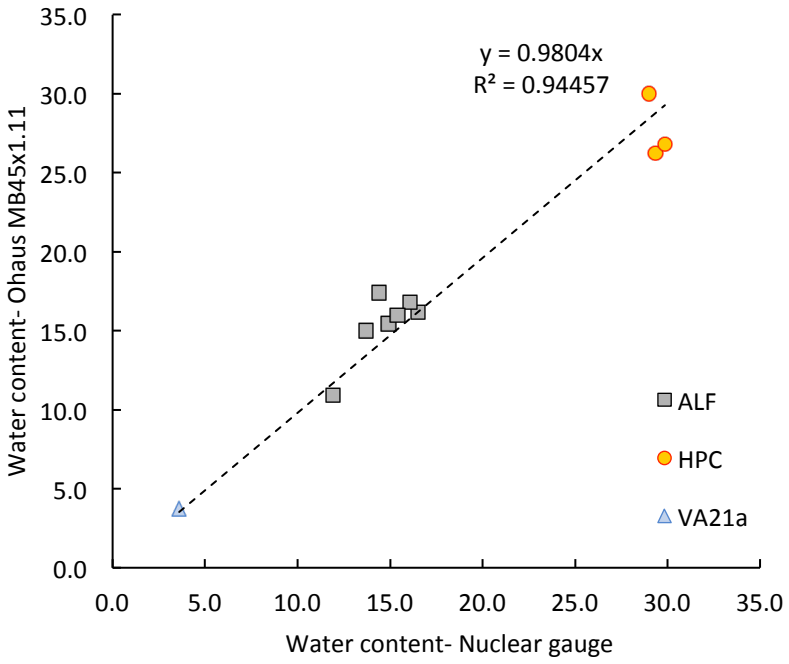

Figure 0.18. GWC by Ohaus MB45 moisture analyzer versus GWC by Nuclear moisture-density gauge.

Plate load testing

Figure 0.19. Static plate load testing.

Table 0-11. Plate load compaction test results.

Location	Set	ks	R^2	Dp	Material	MC	PC	E
[-]	[-]	[kN/m]	[%]	[mm]	[-]	[%]	[%]	[MPa]
Pit I-ALF Loc 9	1	741.2	97.3	6.599	ALF	10.0	84.3	2.8
	2	3437.6	99.8	0.810				12.8
Pit I-ALF Loc 3	1	705.3	88.6	6.507				2.6
	2	3426.2	98.5	0.457				12.8
Pit II-ALF Loc1	1	885.6	99.1	4.503	ALF	15.3	95.6	3.3
	2		-					
Pit II-ALF Loc 2	1	725.2	99.9	6.419				2.7
	2		-					
Pit II-VA21a Loc1	1	2089.6	99.6	1.671	VA21a	5.3	96.4	7.8
	2		-					
Pit II-VA21a Loc 7	1	1806.6	96.8	1.943				6.7
	2		-					
Pit III- HPC- Loc 1	1	4241.0	97.8	0.665	HPC	28.9	96.1	15.8
	2	8261.6	99.5	0.178				30.8

LWD measurements

Table 0-12. LWD testing at Pit 1.

Lift number	Material	LWD testing on constructed layer and time	
0	Crushed stone	7/17/15 2:00 PM	On top of geotextile and crushed stone
1	ALF	7/22/15 1:30 PM	right after compaction
2	ALF	7/24/15 8:00 AM	right after compaction
3	ALF	7/24/15 3:00 PM	2 hr after compaction- Concorrent to plate load test

Table 0-13. LWD testing at Pit 2.

Lift number	Material	LWD testing on constructed layer and time	
5	ALF	7/13/15 10:00 AM	Zorn and Olson only
6	ALF	7/13/15 4:00 PM	1 hr after compaction
		7/14/15 7:30 AM	16 hr after compaction- Concorrent to plate load test
		7/15/15 12:30 PM	21 hr after compaction- Zorn only
7	VA21a	7/15/15 7:30 AM	16 hr after final series of compaction
8	VA21a	7/15/15 12:00 PM	1 hr after compaction
		7/15/15 3:00 PM	5 hr after compaction- Concorrent to plate load test
		7/20/15 1:00 PM	5 days after compaction except Dynatest
		7/24/15 8:30 AM	9 days after compaction

Table 0-14. LWD testing at Pit 3

Lift number	Material	LWD testing on constructed layer and time	
1	HPC	7/17/15 11:00 AM	right after compaction
2	HPC	7/17/15 4:00 PM	Only with Zorn
		7/20/15 9:00 AM	65 hr after compaction
4	HPC	7/20/15 1:00 PM	right after compaction
5	HPC	7/21/15 11:00 AM	right after compaction- Concorrent to plate load test
6	VA21a	7/22/15 10:30 AM	right after compaction
		7/22/15 12:30 PM	1.5 hr after 2nd round compaction
		7/22/15 3:00 PM	4 hr after 2nd round compaction- Concorrent to plate load test
		7/24/15 7:30 AM	45 hr after compaction